Genetic load and extinction in peripheral populations: the roles of migration, drift and demographic stochasticity

Himani Sachdeva[1,2,§], Oluwafunmilola Olusanya[1], Nick Barton[1]

[1] *Institute of Science and Technology Austria, Am Campus 1, Klosterneuburg 3400, Austria.*
[2] *Department of Mathematics, University of Vienna, Vienna 1090, Austria.*
§ Corresponding author

Abstract

We analyse how migration from a large mainland influences genetic load and population numbers on an island, in a scenario where fitness-affecting variants are unconditionally deleterious, and where numbers declines with increasing load. Our analysis shows that migration can have qualitatively different effects, depending on the total mutation target and fitness effects of deleterious variants. In particular, we find that populations exhibit a genetic Allee effect across a wide range of parameter combinations, when variants are partially recessive, cycling between low-load (large-population) and high-load (sink) states. Migration further reduces load in the sink state (by increasing heterozygosity) but increases load in the large-population state (by hindering purging). We identify various critical parameter thresholds at which one or other stable state collapses, and discuss how these thresholds are influenced by the genetic vs. demographic effects of migration. Our analysis is based on a 'semi-deterministic' analysis, which accounts for genetic drift but neglects demographic stochasticity. We also compare against simulations which account for both demographic stochasticity and drift. Our results clarify the importance of gene flow as a key determinant of extinction risk in peripheral populations, even in the absence of ecological gradients.

Keywords: deleterious variants, genetic load, extinction, migration, demographic stochasticity, semi-deterministic approximation

Introduction

Most outcrossing populations carry a substantial masked mutation load due to recessive variants, which can contribute significantly to inbreeding depression in peripheral isolates or after a bottleneck. The extent to which the accumulation of deleterious mutations due to small numbers exacerbates extinction risk in isolated populations has been a subject of long-standing interest [1, 2, 3, 4]. Theory predicts that moderately deleterious mutations contribute the most to genetic load and extinction in small populations [2, 5]; however, the prevalence of such deleterious variants of mild or moderate effect and their dominance values remain poorly characterised, except for a few model organisms [6, 7].

The relative risks posed by mutation accumulation and demographic stochasticity to a population depend crucially on its size, with some theory suggesting that these may be comparable for populations in their thousands [1]. Moreover, environmental stochasticity — catastrophic events, as well as fluctuations in growth rates and carrying capacities, may dramatically lower extinction times [8]. Both demographic and environmental fluctuations, in turn, reduce the effective size of a population, making it more prone to fix deleterious alleles; the consequent

reduction in fitness further depresses size, pushing populations into an 'extinction vortex', which is often characterised by a complex interaction between the effects of genetic drift, demographic stochasticity and environmental fluctuations [9].

Peripheral populations at the edges of species' ranges may be subject to dispersal from the core to an extent which varies over space and time. Moreover, in populations threatened by habitat loss, ranges may be fragmented and individual sub-populations connected to each other via low and possibly declining levels of migration. This makes it necessary to ask: under what condition, can such extinction vortices be arrested by migration, and what are the genetic and demographic underpinnings of this effect, when it occurs?

Migration boosts numbers, mitigating extinction risk due to demographic and environmental stochasticity, or at the very least, allows populations to regenerate after chance extinction. The demographic consequences of migration are especially important in fragmented populations with many small patches [10]: above a critical level of migration, the population may survive as a whole over long timescales even if individual patches frequently go extinct [11, 12].

Migration also influences extinction risk via shifts in the frequencies of fitness-affecting variants: the resultant changes in fitness may decrease or increase population size, thus further boosting or depressing the relative contribution of migration to allele frequency changes within a population, setting in motion a positive feedback which may culminate in extinction (when gene flow is largely maladaptive; e.g., [13, 14]) or population rescue (e.g., if gene flow supplies variation necessary for adaptation to local conditions, or reduces inbreeding load; e.g., [5, 15, 16]).

The maladaptive consequences of migration have largely been explored in the context of gene flow between subdivided or extended populations under spatially varying environmental conditions: here, gene flow typically hinders local adaptation, especially in peripheral populations, leading to 'swamping' and extinction [17]. However, the consequences of gene flow for fitness, and consequently survival, are not always intuitive when the fitness effects of genetic variants are uniformly deleterious (or beneficial) across populations. For example, while gene flow may alleviate inbreeding load by preventing the fixation of deleterious alleles, especially in very small populations, it can also render selection against recessive mutations less effective by increasing heterozygosity. A striking consequence is that under a range of conditions, the fitness of metapopulations is maximised at intermediate levels of migration [18]; more generally, fitness due to recessive variants changes non-monotonically with the degree of population structure, for other kinds of structure as well, e.g., due to selfing [19].

A key consideration is whether or not gene flow is symmetric, i.e., whether some sub-populations are merely influenced by the inflow of genes from the rest of the habitat or if all sub-populations influence the genetic composition of the population as a whole [20]. Asymmetric dispersal is common at the geographic peripheries of species' ranges or on islands. Moreover, populations occupying small patches within a larger metapopulation with a wide distribution of patch sizes, or sub-populations with lower-than-average fitness (and consequently, atypically low numbers) may also experience predominantly asymmetric inflow of genes. Asymmetric gene flow allows for allele frequency differences across the range of a population even in the absence of environmental heterogeneity, e.g., when population sizes (and hence the efficacy of selection relative to drift) vary across the habitat. This, in turn, may generate heterosis or outbreeding depression across *multiple* loci, when individuals from different regions hybridize.

The consequences of asymmetric gene flow are typically simpler to analyse from a conceptual point of view, as they allow us to consider a focal population, while taking the state of the rest of the population as 'fixed'. Such analyses are key to understanding more general scenarios

where genotype frequencies and population sizes across different regions co-evolve.

Here, we analyse the eco-evolutionary dynamics of a single island population subject to migration from a larger mainland population in a scenario where selection across the two populations is uniform, i.e., where fitness is affected by a large number of variants that are unconditionally deleterious. We ask: under what conditions can migration from the mainland alleviate inbreeding load, thus preventing 'mutational meltdown' and extinction of the island population? Further, how are the effects of migration mediated by the genetic architecture of load, i.e., by the genome-wide mutation target and fitness effects of deleterious variants? A key focus is to understand the coupled evolution of allele frequencies (across multiple loci) and population size: to this end, we consider an explicit model of population growth with logistic regulation, where growth is reduced by an amount equal to the genetic load.

While the effects of maladaptive gene flow on marginal populations have been studied under a variety of assumptions [21, 22], there has been little work on how migration affects inbreeding load and survival of such populations under genetically realistic assumptions. In particular, incorporating the polygenic nature of fitness variation into models is crucial, as changes in load (e.g., due to migration) at any locus affect all other loci by effecting changes in population size, which in turn influences the efficacy of selection at all loci.

Model and Methods

We study how deleterious variants affect the survival of a peripheral island population subject to one-way migration from a large mainland. Individuals are diploid and carry L biallelic loci that mutate at rate u per generation between the wildtype and deleterious state. Mutations have the same fitness effects on the mainland and island, i.e., there is no environment-dependent fitness component.

Deleterious variants at different loci affect fitness multiplicatively (no epistasis): individual fitness is given by $e^{-\sum_{j=1}^{L} s_j(X_j+h_jY_j)}$, where X_j (Y_j) equals 1 if the jth locus is homozygous (heterozygous) for the deleterious allele, and is zero otherwise. Here, s_j is the homozygous selective effect and h_j the dominance coefficient for the deleterious allele at locus j. We assume $0 \leq h_j \leq 1/2$, so that deleterious alleles are always (partially) recessive.

In each generation, a random number of individuals (from a Poisson distribution with mean m_0) migrate from the mainland to the island. For simplicity, we assume that the mainland population is large enough that deleterious allele frequencies among migrants (denoted by $\{p_j^{(m)}\}$) are close to the deterministic predictions for a single locus under mutation-selection equilibrium.

We assume density-independent selection on individuals on the island and density-dependent population growth with logistic regulation, where the baseline growth rate is reduced by the genetic load: the population size n_t in any generation t is then Poisson-distributed with mean equal to $n_{t-1}\exp[r_0(1-n_{t-1}/K)]\overline{W}$, where n_{t-1} is the population size in the previous generation, r_0 the baseline growth rate, K the carrying capacity, and $\overline{W}$ the mean genetic fitness. The n_t individuals in the tth generation are formed by randomly sampling $2n_t$ parents (with replacement) from the n_{t-1} individuals in the previous generation with probabilities equal to their relative fitnesses, followed by free recombination between parental haplotypes to create gametes. Diploid offspring are then formed by randomly pairing gametes.

Simulations. We carry out two kinds of simulations: individual-based simulations that explicitly track multi-locus genotypes of all individuals on the island, and simulations that assume

LE (linkage equilibrium) and neglect inbreeding. The latter kind of simulations are computationally less intensive as they only track allele frequencies at the L loci and the size of the population. However, they make two simplifying assumptions: first, that there is no inbreeding so that genotypes at any locus are in Hardy-Weinberg proportions; second, that any statistical associations, e.g., between the allelic states of different loci (linkage disequilibria or LD) or between the probability of identity by descent, and consequently homozygosity, at different loci (identity disequilibria or ID) — are negligible. Then, individual genotypes are simply random assortments of deleterious and wildtype alleles, and can be generated, e.g., in a simulation, by independently assigning alternative allelic states to different loci with probabilities equal to the allele frequencies. Details of the two kinds of simulations are provided in the SI (Appendix A).

Since selection pressures are identical on the mainland and island, any systematic differences in allele frequencies or homozygosity between the two populations across multiple loci (which would generate LD and ID respectively) must arise solely due to differences in population size, which would translate into differences in the efficacy of selection between the mainland and island populations. In general, we expect LD and ID to be negligible when all ecological and evolutionary processes are slow relative to recombination [14]: this may not hold, however, when populations are small (and drift significant), making it necessary to evaluate how statistical associations between deleterious variants affect extinction thresholds. In the rest of the paper, we will only show results of the allele frequency simulations (assuming LE and zero inbreeding); we compare these with individual-based simulations and discuss how LD and ID affect population outcomes in Appendix B (SI).

Joint evolution of allele frequencies and population size. Assuming LE and no inbreeding, the evolution of the island population is fully specified by how allele frequencies $\{p_j\}$ and the population size n co-evolve in time t. If changes due to evolutionary and ecological processes per generation are small, we can describe this co-evolution in continuous time. We rescale all rates by the baseline growth rate r_0 and population sizes by the carrying capacity K. This yields the following dimensionless parameters: $\tau{=}r_0t$, $S{=}s/r_0$, $M_0{=}m_0/(r_0K)$, $U{=}u/r_0$, $N_t{=}n_t/K$ and an additional parameter $\zeta{=}r_0K$ which governs the strength of demographic fluctuations. The joint evolution of allele frequencies $\{p_j\}$ and the scaled population size N in continuous time is described by the following equations:

$$\begin{aligned}
\frac{dp_j}{d\tau} &= -\frac{p_jq_j}{2}\frac{\partial R_g}{\partial p_j} + U(q_j - p_j) + \frac{M_0}{N}(p_j^{(m)} - p_j) + \lambda_{p_j} \\
\frac{dN}{d\tau} &= N\,[1 - N - R_g] + M_0 + \lambda_N \qquad \text{where} \quad R_g = \sum_{j=1}^{L} S_jp_j(2h_jq_j + p_j)
\end{aligned} \tag{1}$$

Here $\mathbb{E}$ denotes the mean; we have λ_N and λ_{p_j} to be random processes satisfying $\mathbb{E}[\lambda_{p_j}]{=}\mathbb{E}[\lambda_n]{=}0$, $\mathbb{E}[\lambda_N(t)\lambda_N(t')]{=}\frac{N(t)}{\zeta}\delta(t{-}t')$ and $\mathbb{E}[\lambda_{p_j}(t)\lambda_{p_j}(t')]{=}\frac{1}{\zeta}\frac{p_j(t)q_j(y)}{N(t)}\delta(t{-}t')$. The four terms in the first equation correspond (in order of appearance) to changes in allele frequency due to selection, mutation, migration and drift. Note that the strength of migration is inversely proportional to the size of the population, reflecting the stronger (relative) effect of migration on the genetic composition of smaller, as opposed to larger, island populations. The second equation describes the evolution of population size: the first term describes changes in population size under logistic growth, where the growth rate is reduced by a factor proportional to the log mean fitness (i.e., the genetic load); the second term captures the effect of migration; the third term corresponds to demographic fluctuations (whose variance is proportional to N, the size of the population). These equations captures a key feature of polygenic eco-evolutionary dynamics —

namely, that the evolution of allele frequencies at different loci is *coupled* via their dependence on a common N, which in turn is influenced by the degree of maladaptation at all loci via R_g. Thus, allele frequencies do *not* evolve independently, even though allelic states at different loci are statistically independent at any instant (under LE).

For *fixed* N, we can write down the joint distribution of allele frequencies at equilibrium, which is a product of the distributions at individual loci (under LE and IE). For a given locus j, this is simply Wright's distribution (expressed in terms of scaled parameters):

$$\psi(p_j|N) \propto p_j^{4\zeta NU+4\zeta M_0 p_j^{(m)}-1}(1-p_j)^{4\zeta NU+4\zeta M_0(1-p_j^{(m)})-1}e^{-2\zeta NSp_j[p_j+2h(1-p_j)]} \tag{2}$$

Integrating over this distribution yields the expected allele frequency $\mathbb{E}(p_j|N)$ and the expected heterozygosity $\mathbb{E}(2p_jq_j|N)$ at any locus, and thence the expected total load $\mathbb{E}(R_g|N)=\sum_j S_j[\mathbb{E}(p_j|N)-(1/2-h)\mathbb{E}(2p_jq_j|N))]$ (scaled by the baseline growth rate r_0) for fixed N.

However, in reality, N is not fixed and will fluctuate — both due to random fluctuations in fitness (due to the underlying stochastic fluctuations of allele frequencies at equilibrium) and due to random fluctuations in reproductive output of individuals (demographic stochasticity). Thus, N itself follows a distribution. While we can write down an equation for the stochastic co-evolution of population sizes and allele frequencies, no explicit solution for the joint equilibrium distribution is possible unless mutation rates are strictly zero (as assumed by [14]). Thus, we must employ various approximations to describe the coupled dynamics of N and $\{p_j\}$.

Approximate semi-deterministic analysis. We expect the population size distribution to be sharply peaked around one or more values $\{N_*\}$ if demographic fluctuations are weak (i.e., for high values of $\zeta=r_0K$) and if fluctuations in mean fitness are also weak (i.e., for large L). Such sharply-peaked distributions correspond to a scenario where populations only transition rarely between alternative peaks, i.e., where the alternative peaks $\{N_*\}$ of the size distribution represent 'metastable' states, allowing allele frequencies sufficient time to equilibrate at any N_*. Under these conditions, it is reasonable to expect that the genetic load would be close to the expected value $\mathbb{E}(R_g|N_*)$ under mutation-selection-drift-migration balance (*given* N_*) when populations are in one of the alternative metastable states, though not necessarily while they transition between states. In order to determine $\{N_*\}$, we postulate that these must represent stable equilibria of the population size dynamics, neglecting demographic stochasticity and assuming that mean fitness (given N_*) is close to the expectation under mutation-selection-drift-migration balance for that N_*. Then we have:

$$0=N_*\,(1-N_*-\mathbb{E}[R_g|N_*])+M_0 \qquad 1-2N_*-\mathbb{E}[R_g|N_*]-N_*\left.\frac{d\mathbb{E}[R_g]}{dN}\right|_{N=N_*}<0 \tag{3}$$

The equality follows from eq. (1), by setting the third (noise) term to zero and assuming that R_g is close to its *equilibrium* expectation $\mathbb{E}(R_g|N_*)$ given N_*. The second inequality expresses the condition for N_* to be a stable equilibria: this means that populations starting at an arbitrary N in the vicinity of N_* would evolve towards this equilibrium size. Equation (3) can be solved numerically to obtain the equilibria $\{N_*\}$, which, under the above assumptions, will be close to the peaks of the population size distribution. As we see below, depending on the parameter regime, there may be one or two stable equilibria of eq. (3), corresponding to population size distributions that are unimodal or bimodal. Bifurcations (i.e., critical parameter thresholds where one of the two stable equilibria vanishes) thus correspond to qualitative transitions in the state of the population.

We will refer to the analysis above as a 'semi-deterministic analysis' as it accounts for the stochastic effects of genetic drift on allele frequencies and load (via the expectation $\mathbb{E}[R_g|N_*]$) but neglects demographic stochasticity. In general, we expect the semi-deterministic analysis to become more accurate for larger $\zeta{=}r_0K$ (see also Appendix B, SI), since $1/\zeta$ governs the strength of demographic fluctuations [14].

Results

Metastable populations and extinction times in the absence of migration

We first consider peripheral populations in the absence of migration. Such populations necessarily become extinct in the long run: however, depending on the mutation target for deleterious mutations (relative to the baseline growth rate r_0), the fitness effects of mutations and the carrying capacity of the island, extinction times may be very long and populations metastable.

We can use eq. (3) to gain intuition for the conditions under which population numbers are metastable even without migration. Setting $M_0{=}0$, it follows that there is always an equilibrium at $N{=}0$ (corresponding to extinction): this equilibrium is stable for $L(S/2)(1/2{+}h){>}1$ where $S{=}s/r_0$, and unstable otherwise. There may exist another equilibrium at $N_*{=}1{-}\mathbb{E}[R_g|N_*, M_0{=}0]$; the population size N_* is positive (and hence biologically meaningful) only if $\mathbb{E}[R_g|N_*, M_0{=}0]{<}1$, i.e., the equilibrium genetic load is lower than the baseline growth rate.

Since the equilibrium load $\mathbb{E}[R_g|N_*, M_0{=}0]$ depends on 4 independent parameters, which we can choose as $\zeta S{=}Ks$, $\zeta U{=}Ku$, h and $2LU{=}2L(u/r_0)$, mapping the conditions for metastability boils down to asking: in the absence of demographic fluctuations, where in this 4-dimensional parameter space, can we find populations with a non-zero equilibrium size or sufficiently low load (fig. 1(a))? In reality, there is a fifth parameter $\zeta{=}r_0K$, which governs the extent of demographic stochasticity: thus, all other parameters being equal, extinction times will be higher when demographic stochasticity is weaker, i.e., r_0K larger (fig. 1(b)).

For simplicity, we assume that deleterious alleles anywhere on the genome have the same selective effects and dominance coefficients; this assumption is relaxed in Appendix D, SI. We use Ks_c to denote the critical selection strength per homozygous deleterious allele (scaled by the carrying capacity K), such that a non-zero equilibrium N_* exists for $Ks{>}Ks_c$ but not for $Ks{<}Ks_c$. Figure 1(a) shows Ks_c as a function of $2LU{=}2L(u/r_0)$, the total mutation rate relative to the baseline growth rate, for different values of Ku (different colors) for nearly recessive ($h{=}0.02$; solid lines) and additive ($h{=}0.5$; dashed lines) alleles.

For populations to be metastable, the total genetic load must be less than the baseline growth rate. The total load scales with the mutation target L; the load per locus is $\sim 2u$ for strongly deleterious variants ($u/hs{\ll}1$ and $Ks{\gg}1$). At lower values of Ks, drift will typically inflate load above this deterministic expectation when deleterious alleles are additive ($h{\sim}1/2$) but may also reduce load (via more efficient purging) when alleles are recessive ($h{\sim}0$). This is reflected in figure 1(a): the threshold Ks_c required to maintain metastable populations is higher for additive deleterious alleles (dashed lines) than recessive alleles (solid lines). Moreover, since genetic load in this drift-dominated regime depends only weakly on the mutational input Ku, the threshold Ks_c is largely independent of Ku (different colors). Finally, we note that for all parameter combinations, the threshold Ks_c increases as the mutation target becomes larger: this simply reflects the fact that for the total load to be less than the baseline growth rate, the load per locus must be lower (requiring stronger selection) if deleterious variants segregate at a greater number of loci. Accordingly, for very large mutation targets $2LU{=}2L(u/r_0){\gtrsim}1$,

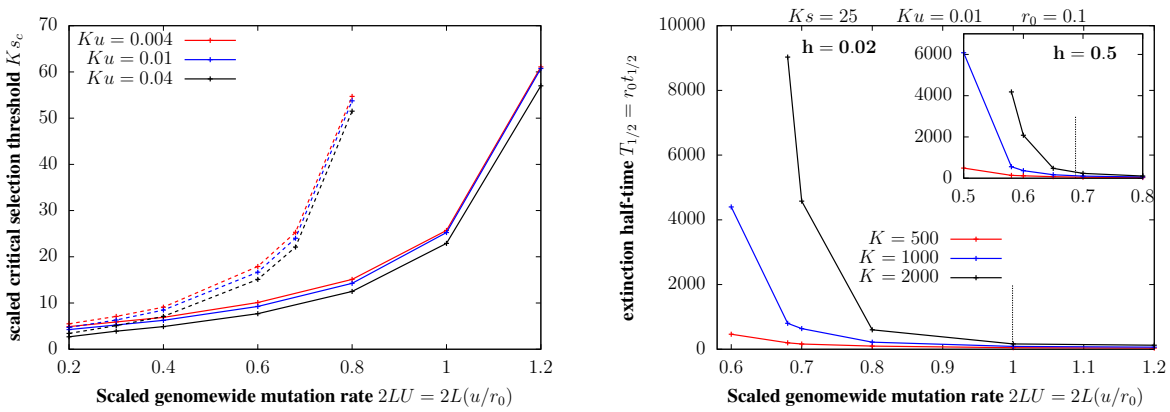

(a) (b)

Figure 1: Population outcomes with zero migration. (A) Scaled critical selection threshold Ks_c, above which populations are metastable, as a function of the scaled mutation target $2LU$=$2L(u/r_0)$ for different values of Ku (different colors) for nearly recessive (h=0.02; solid lines) and additive (h=0.5; dashed lines) alleles. A non-zero equilibrium population size N_*=$1-\mathbb{E}[R_g|N_*]$ exists for $Ks>Ks_c$ but not for $Ks<Ks_c$. This selection threshold is calculated using eq. (3) by neglecting demographic stochasticity, and thus strictly provides a criterion for stable populations in the limit ζ=$r_0K\to\infty$. (B) The scaled extinction half-time $T_{1/2}$=$r_0t_{1/2}$ (see text for definition) as a function of $2LU$ for various K (different colors) for nearly recessive (h=0.02; main plot) and additive alleles (inset). The carrying capacity is increased while proportionately decreasing s, u and increasing L, such that Ks=25, Ku=0.01 and $2LU$=$2L(u/r_0)$ remain unchanged; increasing K thus has the sole effect of weakening demographic stochasticity. Extinction times are computed from simulations of allele frequencies and population size (under LE and IE) with r_0=0.1.

the total load will exceed r_0 (and populations will fail), irrespective of the strength of selection against deleterious mutations.

The critical selection thresholds for metastability shown in fig. 1(a) are computed by neglecting demographic stochasticity, i.e., by assuming r_0K to be very large. However, for moderate r_0K, stochastic fluctuations in reproductive output from generation to generation may accelerate extinction: this effect can be especially significant in smaller populations as these tend to fix more deleterious alleles, which further reduces fitness and size, thus rendering populations even more vulnerable to stochastic extinction.

To investigate how demographic stochasticity contributes to extinction, we simulate (assuming LE and zero inbreeding) populations that are characterised by the same values of Ks, Ku, $2LU$=$2L(u/r_0)$ and h, but reside on islands with different carrying capacities K. Populations are initially perfectly fit, but accumulate deleterious variants over time, eventually becoming extinct due to the combined effects of genetic load (which reduces growth rates) and demographic stochasticity. Figure 1(b) shows the extinction 'half-time' $T_{1/2}$=$r_0t_{1/2}$ (scaled by the baseline growth rate r_0) — the time by which precisely half of all simulation replicates are extinct, as a function of $2LU$ for various K (different colors) for nearly recessive (main plot) and additive alleles (inset). Dashed vertical lines indicate the threshold $2LU$ above which metastable populations (with N_*=$1-E[R_g|N_*]>0$) cannot exist (even for large r_0K).

We find that extinction times increase with increasing K for all parameters. However, for parameter combinations that correspond to extinction in the large r_0K limit (i.e., to the right of the dashed lines), this increase is approximately linear in K, while for parameters leading to metastability in the large r_0K limit (left of dashed lines), this increase is faster than linear. In fact, in the metastable regime, even with a carrying capacity K of a few thousand individuals, demographic stochasticity will be sufficiently weak and extinction times large enough that

isolated populations can persist over geological timescales: for these parameter regimes, it is environmental fluctuations (which our model ignores), rather than mutation load or demographic stochasticity, that will be the main determinant of extinction risk.

Effect of migration on equilibrium population sizes and genetic load

We now ask: how does migration from a large mainland influence population dynamics on the island, for different architectures of genetic load, i.e., given certain selective effects and dominance coefficients of deleterious alleles? As before, we focus on the case where all deleterious alleles have equal selective effects and dominance values, relegating the discussion of more general scenarios, where alleles with different fitness effects segregate, to the SI (Appendix D).

We first analyse the two extremes: nearly recessive (h=0.02 in fig. 2) and additive (h=0.5) alleles, to identify critical parameter thresholds associated with qualitative changes in population outcomes. In the next section, we also consider how these thresholds depend on the level of dominance of deleterious alleles (fig. 3). Figure 2 illustrates the effect of migration on population sizes and load on the island for three parameter combinations, corresponding to weakly deleterious ($Ks<Ks_c$; left column), moderately deleterious ($Ks\gtrsim Ks_c$; middle) and strongly deleterious ($Ks\gg Ks_c$; right) nearly recessive alleles (h=0.02). Recall that Ks_c is the selection threshold (obtained by neglecting demographic stochasticity) such that populations rapidly go extinct in the absence of migration for selection strengths weaker than Ks_c, but can be metastable (even without migration) for $Ks>Ks_c$ and $r_0K\to\infty$ (fig. 1).

Figures 2(a)-2(c) show population sizes corresponding to stable equilibria of eq. (3) as a function of m_0, the number of migrants per generation, for $Ks<Ks_c$, $Ks\gtrsim Ks_c$ and $Ks\gg Ks_c$. The insets show the equilibrium load vs. m_0. Since these equilibria are calculated by numerically solving eq. (3), they represent *semi-deterministic* predictions, i.e., they neglect the effects of demographic stochasticity but account for the effects of drift, assuming that populations spend enough time in any metastable state that the distribution of allele frequencies can equilibrate. Figures 2(d)-2(f) show the stochastic distribution of the scaled population size $N=n/K$ (at equilibrium) as obtained from allele frequency simulations (assuming LE and zero inbreeding), for various m_0, in the three parameter regimes. Figures 2(g)-2(i) show the corresponding time series $N(t)$ over an arbitrary period, after the population has equilibrated.

Weakly deleterious recessive alleles. For $Ks<Ks_c$, there exists a single stable equilibrium at all migration levels (fig. 2(a)), with the corresponding population size approaching zero as migration becomes rarer. Accordingly, the stochastic distribution of N exhibits a single peak for all m_0 (fig. 2(d)). An increase in migration causes the genetic load to decrease (inset, fig. 2(a)) and the population size to increase. The stochastic distribution of population sizes is approximately exponentially distributed for low values of m_0 (corresponding to a sink state), but shifts towards higher values of N as m_0 increases, and is approximately normally distributed about the deterministic equilibrium N_* (indicated by empty triangles in fig. 2(d)) for large m_0.

Increasing migration has two effects in this case: it reduces genetic load, typically by reducing homozygosity— a *genetic* effect, but also increases population numbers— a *demographic* effect. The genetic effect of migration, i.e., the dependence of the expected load $\mathbb{E}(R_g|N)=\sum_j S_j[\mathbb{E}(p_j|N)-(1/2-h)\mathbb{E}(2p_jq_j|N)]$ on m_0, can be further decomposed into effects on the expected frequencies $\mathbb{E}(p_j|N)$ and expected heterozygosity $\mathbb{E}(2p_jq_j|N)$ of deleterious alleles. For weakly deleterious recessive alleles, the expected frequency decreases with increasing migration for low m_0, is minimum at intermediate m_0, and then increases as m_0 increases further (not shown). However, genetic load still decreases monotonically with increasing migration

(inset, fig. 2(a)), due to the much sharper increase in heterozygosity with migration.

Strongly deleterious recessive alleles. For $Ks \gg Ks_c$, there exist *two* stable equilibria of the semi-deterministic population size dynamics (eq. (3)) at low levels of migration: population sizes and values of load corresponding to these two equilibria are shown in blue and red in fig. 2(c). One equilibrium (blue lines in fig. 2(c)) corresponds to a sink state with the associated population size approaching zero as $m_0 \to 0$. The other equilibrium (depicted in red) corresponds to a large population, which can persist at finite fraction of carrying capacity even as migration becomes exceedingly rare, i.e., has size N_*, which approaches $1-\mathbb{E}[R_g|N_*, M_0=0]>0$ as $m_0 \to 0$.

The existence of two stable equilibria at low m_0 translates into *bimodal* population size distributions (in black and brown in fig. 2(f)), with one peak close to extinction and the other at the semi-deterministic N_* (depicted by filled triangles). Population size $N(t)$ also exhibits characteristic dynamics (see time series in black and brown in fig. 2(i)): populations tend to remain 'stuck' in either the sink state or the large-population state for long periods of time, typically exhibiting rather small fluctuations about the characteristic sizes associated with either state, and only transitioning rarely between states.

The sink state and large-population state can also be thought of as "high-load" (i.e., genetic load greater than the baseline growth rate r_0) and "low-load" (genetic load less than r_0) states. Thus, in this parameter regime, populations exhibit a genetic Allee effect, wherein load is sufficiently low and net growth rates positive only above a threshold population size: populations starting at small numbers cannot grow deterministically, even though large populations can maintain themselves, at least in the absence of demographic fluctuations. Transitions between the sink (high-load) and large-population (low-load) states are thus inherently stochastic, arising due to demographic fluctuations (which are aided by higher levels of migration) rather than due to a systematic drive towards the alternative state.

Changes in m_0 have qualitatively different effects on the two states: at low m_0, increasing migration reduces load and thus increases numbers in the sink state (blue curve), but has the *opposite* effect on the large-population equilibrium (red curves). This is due to the non-monotonic dependence of the frequency of deleterious recessive alleles on population size: increasing size causes drift to become weaker relative to selection but also reduces homozygosity, so that fewer deleterious alleles are exposed to selection; frequencies are thus minimum at intermediate population sizes, reflecting the tension between these two opposing effects. In small sink populations, migration from the continent reduces homozygosity as well as deleterious allele frequencies, thus reducing load. However, in larger populations, increasing migration reduces the homozygosity but raises the frequency of deleterious alleles (since deleterious alleles are purged less efficiently in very large mainland populations than in intermediate-sized or large island populations); the overall effect of migration is thus to increase load in the large-population state.

Above a critical migration threshold, which we denote by $m_{c,1}$, the sink equilibrium vanishes. Thus, for $m>m_{c,1}$, populations always have a positive growth rate and reach a finite fraction of carrying capacity, regardless of starting size. As before, this qualitative change in the (semi-deterministic) population size dynamics at a critical migration level has its analog in a qualitative change in the stochastic distribution of population sizes (fig. 2(f)): increasing migration causes the population size distribution to change from bimodal to unimodal (with a sole peak at the large-population equilibrium $N_*=1-\mathbb{E}[R_g|N_*]$)). At higher migration rates, i.e., as we approach to the critical migration threshold $m_{c,1}$ starting from low m_0, turnover between the sink and large-population states becomes more rapid— note the shorter intervals between transitions in the brown vs. black time series in fig. 2(i).

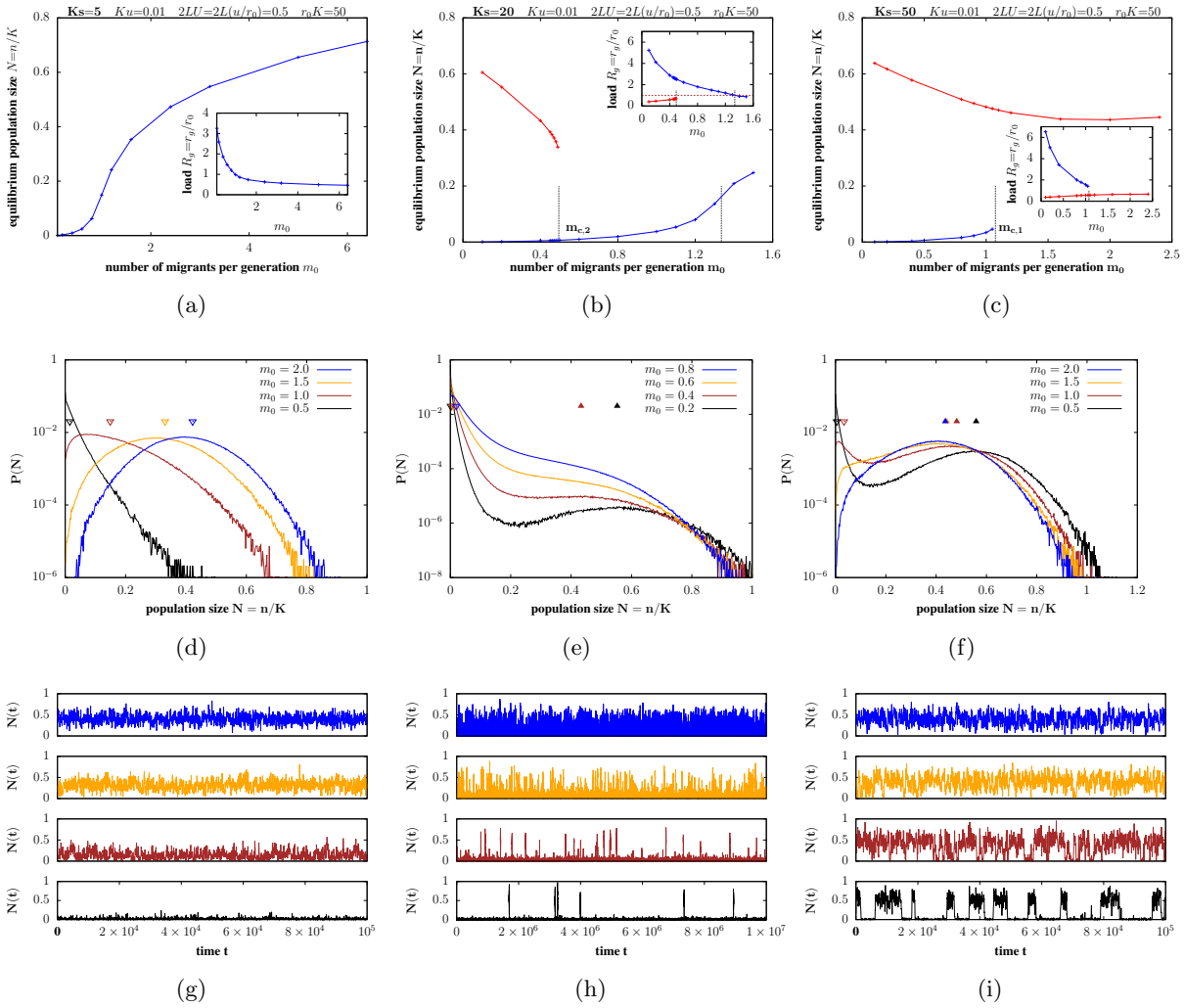

Figure 2: Effect of migration on equilibrium population sizes and load for weakly deleterious ($Ks<Ks_c$; left column), moderately deleterious ($Ks\gtrsim Ks_c$; middle) and strongly deleterious ($Ks\gg Ks_c$; right) alleles. (A)-(C) Population size (main plots) and genetic load (inset), corresponding to one or more stable equilibria, vs. m_0, the number of migrants per generation. Equilibria are obtained by numerically solving eq. (3) (semi-deterministic predictions). Blue lines represent the sink equilibrium (with an associated population size that tends to zero as $m_0\to 0$); red lines represent the large-population equilibrium (with non-zero population size in the $m_0\to 0$ limit). The thresholds $m_{c,2}$ (2B) and $m_{c,1}$ (2C) represent critical migration thresholds at which the sink or the large-population equilibrium vanishes. The threshold $m_{c,3}$ (2B) is the critical migration level at which the (scaled) load associated with the sink state becomes less than 1. (D)-(F) Equilibrium probability distributions of the scaled population size $N=n/K$ for various values of m_0, as obtained from simulations (under LE and IE) in the three parameter regimes. The filled and empty triangles indicate the population sizes corresponding to alternative equilibria as predicted by the semi-deterministic analysis. (G)-(I) Time series $N(t)$ vs. t over an arbitrary period after equilibration in the three regimes. All plots show results for: Ku=0.01, $2LU$=$2L(u/r_0)$=0.5, ζ=r_0K=50, h=0.02 and Ks=5, 20, 50 for the left, middle and right columns respectively (the critical threshold is $Ks_c\sim$7.65). In addition, for the simulations (plots D-I), we use r_0=0.1.

Moderately deleterious recessive alleles. Consider now the case where selection is stronger than the threshold Ks_c but not too strong, i.e., $Ks \gtrsim Ks_c$ (middle column in fig. 2). As in the $Ks \gg Ks_c$ case, there exist two alternative stable equilibria at low migration levels, one corresponding to the sink state (blue lines in fig. 2(b)) and the other to the large-population state (red lines). As before, increasing migration alleviates inbreeding load and increases population size in the sink state but elevates load (by hindering purging) and decreases population size in the large-population state. Unlike in the $Ks \gg Ks_c$ state, the latter effect is much stronger: thus, above a critical migration threshold, which we denote by $m_{c,2}$, it is the large-population equilibrium that vanishes, so that there is only a single (sink) equilibrium for $m > m_{c,2}$.

The analogous change in the population size distribution with increasing migration (fig. 2(e)) is somewhat subtle: for the lowest value of m_0 (black), the distribution is clearly bimodal, with most of the weight close to $N=0$ (sink state) and a very small peak at the large-population equilibrium. As migration increases, the distribution of sizes associated with the sink state widens, while the peak corresponding to the large-population equilibrium shifts towards lower values of N (e.g., brown plot). At high migration levels (orange and blue plots), there is no longer a distinct second peak and only the sink state persists. In this state, the genetic load exceeds r_0 *on average*; however, the distribution of genetic load and the corresponding distribution of sizes is quite wide.

If migration increases further, then the average load associated with the sink state continues to fall, until at a third threshold (denoted by $m_{c,3}$, here $\sim$1.33), the load again becomes lower than the baseline growth rate r_0 or, alternatively, scaled load $R_g = r_g/r_0$ less than 1 (denoted by a dashed line in fig. 2(b)). Thus, for $m_0 > m_{c,3}$, populations can grow, starting from small numbers, and reach a finite fraction of carrying capacity. However, this state is qualitatively distinct from the large-population state at higher values of Ks, in that populations are highly dependent on migration and would rapidly collapse (due to the fixation of deleterious alleles) if cut off from the mainland population.

Population size dynamics (fig. 2(h)) are characterised, as in the $Ks \gg Ks_c$ case, by occasional transitions between the sink state and the large-population state for low values of m_0 (black), with transitions becoming more frequent with increasing m_0 (orange). The timescales of transitions are much larger than in the $KS \gg Ks_c$ case (note the values on the x-axis); thus transitions are unlikely to occur over realistic timescales, and populations will typically be observed in the sink state. At higher migration levels, there are no obvious transitions, with population sizes and load fluctuating (with some skew) about a mean value.

Additive alleles. With additive effects ($h \sim 0.5$), any deleterious allele experiences the same selective disadvantage, irrespective of whether it appears in the heterozygous or homozygous state: thus, there is no purging in smaller populations (which have higher homozygosity) and allele frequencies decrease monotonically with increasing population size. As a result, migration from the larger mainland population always decreases load (by decreasing the deleterious allele frequency) and increases the size of the island population.

This implies that there are only two qualitatively distinct regimes: with weakly deleterious alleles (Ks less than the corresponding Ks_c; see fig. 1(a)), populations tend to extinction as migration declines. There is a single equilibrium of the semi-deterministic population size dynamics for all m_0 or analogously, a single peak of the stochastic population size distribution, which shifts towards higher sizes as m_0 increases.

For strongly deleterious alleles ($Ks > Ks_c$), population sizes and load are largely insensitive to migration, since populations can always grow, starting from small numbers, at least when

demographic stochasticity is unimportant (i.e., for large r_0K). With smaller r_0K, population sizes and load exhibit a weak dependence on migration even with $Ks>Ks_c$, since demographic stochasticity may depress population sizes and inflate the effects of drift, especially at low numbers. Moreover, in this regime, populations are also prone to stochastic extinction for $m_0<1/2$ [14], such that population size distributions are inherently bimodal. Thus, where demographic stochasticity is significant, a low level of migration may be needed for stable populations even with strong selection against additive alleles.

Although we have analysed the special case where all deleterious alleles have equal selective effects and dominance coefficients, the analysis (based on eq. (3)) also applies to more realistic genetic architectures with a distribution of effects. In Appendix D (SI), we consider examples where a fraction of deleterious mutations are additive and the remaining fraction recessive. We also compare the results of allele frequency simulations shown here with those of full-individual based simulations (Appendix C, SI). These show fairly close agreement, suggesting that LD and ID do not significantly affect allele frequency dynamics, at least for the typical parameter values considered here: this is also consistent with earlier work, which suggests only a modest effect of disequilibria on background selection in sub-divided populations under soft selection [19].

Disentangling genetic vs. demographic effects of migration on recessive alleles.

In summary, given a mutation target $2LU\lesssim 1$ and assuming equal-effect loci, there is a critical selection threshold Ks_c such that large populations are metastable in the limit of zero migration for $Ks>Ks_c$ but not for $Ks<Ks_c$. For $Ks>Ks_c$, there is a genetic Allee effect at low migration rates and with partially recessive alleles: while populations can maintain themselves at large numbers, they cannot grow from small numbers, and only persist as demographic sinks until a chance fluctuation pushes numbers to sufficiently high values that load can be purged and the alternative (large-population) equilibrium attained. Moreover, with low dominance values ($h\lesssim 0.15$), there is a second threshold $Ks_{c,2}$ (see below) which separates parameter regimes characterised by qualitatively different effects of migration on population outcomes: for $Ks>Ks_{c,2}$, increasing migration destabilizes the sink state, so that only the large-population state persists above a threshold $m_{c,1}$; for $Ks_c<Ks<Ks_{c,2}$, increasing migration destabilizes the large-population state, so that only the sink state persists above a critical migration threshold $m_{c,2}$. However, such migration-fed sink populations can be fairly large: above a critical threshold $m_{c,3}$, populations may have sufficient heterozygosity to again attain a low-load ($r_g<r_0$) state.

We now ask: to what extent can we attribute such qualitative changes in population outcomes with changing migration to the genetic vs. demographic effects of migration? As before, one approach is to compare critical thresholds for populations with the same scaled parameters Ks, Ku, $2LU=2L(u/r_0)$ and h, while increasing the carrying capacity K (simultaneously increasing L and lowering u, s). In the large K limit, the demographic effects of migration (which depend on the dimensionless parameter $M_0=m_0/(r_0K)$; see eq. (1)) can be neglected, while the genetic effects of migration on load (which depend on Ks, Ku and m_0) remain important.

Figure 3 shows these comparisons for two dominance values — $h=0.02$ (figs. 3(a), 3(b)) and $h=0.1$ (figs. 3(c), 3(d)). Note that we only consider predictions of the semi-deterministic analysis (eq. (3)), which assumes that population sizes are sharply clustered around the peaks of the distribution and transitions between peaks are infrequent. This assumption clearly breaks down close to transition thresholds (e.g., see figs. 2(e), 2(f)); thus, thresholds observed in simulations may differ somewhat from semi-deterministic predictions (details in Appendix B, SI). Moreover, the semi-deterministic analysis neglects all demographic stochasticity, and thus does not account for the fact that changes in K will affect not just the (systematic) demographic

effect of migration but also the (stochastic) effect of demographic fluctuations. Nevertheless, the semi-deterministic analysis is useful as it allows us to explore qualitative dependencies of critical thresholds on the underlying parameters without resorting to time-consuming simulations.

Figures 3(a) and 3(c) show the critical selection thresholds Ks_c (as in fig. 1(a)) and $Ks_{c,2}$ as a function of the scaled mutation target $2LU{=}2L(u/r_0)$ for various carrying capacities for the two values of h (with Ks, Ku, $2LU{=}2L(u/r_0)$ held constant, as K is varied). The threshold Ks_c, which relates to population outcomes in the zero migration limit, is (by definition) independent of K in the semi-deterministic setting, as increasing K merely weakens the demographic effects of migration. The threshold $Ks_{c,2}$ decreases as K decreases, i.e., as the demographic effects of migration become stronger. This means that when alleles are moderately deleterious, i.e., characterised by a certain intermediate value of Ks, populations are stabilized (i.e., rescued from recurrent collapse into the high-load sink state) by increasing migration more easily on *smaller* islands, where the demographic effects of migration are stronger.

Figure 3(b) and 3(d) show the critical migration thresholds $m_{c,1}$, $m_{c,2}$ and $m_{c,3}$ vs. $2LU$ for a given Ks value (chosen to be 50). Here, with $h{=}0.02$ for example (fig. 3(b)), increasing migration causes the sink state to vanish for $2LU{\lesssim}0.5$, but degrades the large-population (low-load) state for $2LU{\gtrsim}0.5$. The threshold $m_{c,1}$ (solid lines) is highly sensitive to K: populations can be stabilized at a finite fraction of carrying capacity at much lower levels of migration on smaller islands (given Ks, Ku), suggesting a key role of the demographic effects of migration. We can obtain an explicit expression for the threshold $m_{c,1}$ in the limit $K{\to}\infty$ (where the demographic effects of migration are negligible):

$$m_{c,1}{=}\frac{LSp^{(m)}{-}1}{4[1{-}LSp^{(m)}(p^{(m)}{+}2h(1{-}p^{(m)}))]} \qquad \text{as} \quad K{\to}\infty \tag{4}$$

Interestingly, this threshold depends only on the load, $LSp^{(m)}(p^{(m)}{+}2h(1{-}p^{(m)}))$, and breeding value, $LSp^{(m)}$, among migrants, and is independent of Ks and Ku: this simply reflects the fact that the genetic composition, and hence the growth rate, of a very small population is determined primarily by migration (and not selection). Thus, the critical level of migration required to prevent a genetic Allee effect (i.e., to ensure positive growth rates, starting from low numbers) in the limit of very large carrying capacities is also independent of Ks and Ku.

The threshold $m_{c,2}$, which signals the collapse of the large-population state, is less sensitive to K: this is consistent with our expectation that demographic effects of migration should be less important when numbers are larger. There is, nevertheless, a moderate decrease in $m_{c,2}$ with K, which can be rationalised as follows: the (detrimental) genetic effects of migration on the large-population state are more effectively compensated by its demographic effects when islands are smaller (lower carrying capacity), allowing the large-population state to persist despite higher levels of migration on such islands. Finally, the third threshold $m_{c,3}$, which signals the emergence of a migration-dependent low-load state (at large $2LU$) is also highly sensitive to the demographic effects of migration, and becomes unrealistically high in the large K limit, where increasing migration can only shift allele frequencies but has little effect on population numbers (relative to carrying capacity).

A comparison of the top and bottom rows in fig. 3, which correspond respectively to $h{=}0.02$ and $h{=}0.1$, reveals that as deleterious alleles become less recessive (larger h), the parameter regime in which increasing migration eliminates the large-population equilibrium shrinks drastically, and only emerges for very high genome-wide mutation rates — with $h{=}0.1$, the second threshold $Ks_{c,2}$ exists only for $2LU{\gtrsim}0.8$ in fig. 3(c). This is consistent with the fact that purging of recessive mutations in smaller populations (which allows them to evolve significantly

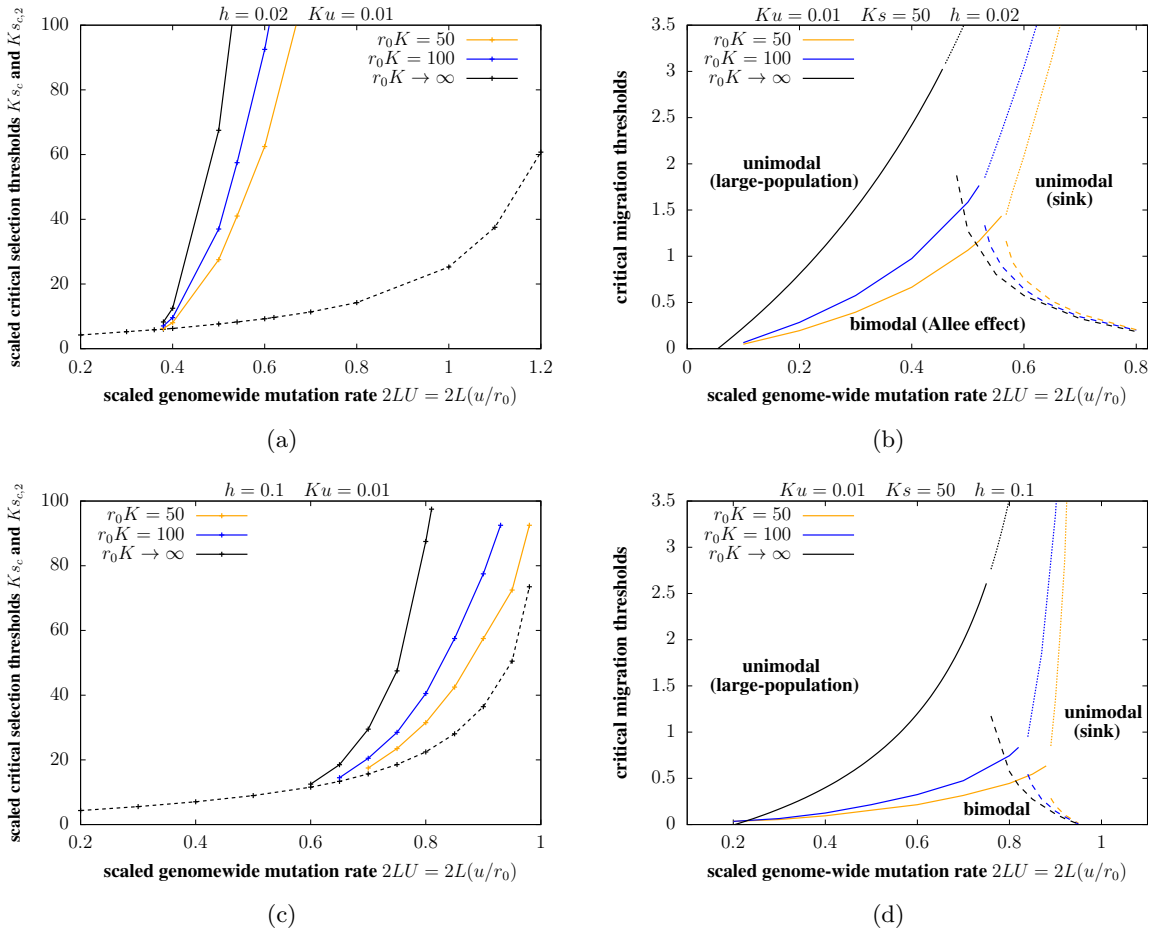

Figure 3: Semi-deterministic predictions for critical thresholds with and without accounting for demographic effects of migration. (A) and (C): Critical selection thresholds Ks_c (dashed line) and $Ks_{c,2}$ (solid lines) as a function of the scaled mutation target $2LU$=$2L(u/r_0)$ with (A) h=0.02 and (C) h=0.1, for r_0K=50, r_0K=100 and for $r_0K \to \infty$ (in which limit migration has negligible demographic effects). The parameter r_0K, which governs the magnitude of the demographic effect of migration (via the term M_0=$m_0/(r_0K)$) is varied by changing K, while simultaneously varying s, u and L such that Ks, Ku and $2LU$=$2L(u/r_0)$ are constant (so that the genetic effects of migration remain unchanged). The threshold Ks_c is such that populations rapidly go extinct for Ks<Ks_c in the limit of zero migration, but are metastable for Ks>Ks_c, if starting from large but not small sizes (so that there is a genetic Allee effect). The second threshold $Ks_{c,2}$ is such that increasing migration destabilizes the sink state for Ks>$Ks_{c,2}$, but destabilizes the large-population state for Ks_c<Ks<$Ks_{c,2}$. The threshold Ks_c is independent of migration, but $Ks_{c,2}$ increases as r_0K increases, i.e., as the demographic effect of migration becomes weaker. (B) and (D) The critical migration thresholds $m_{c,1}$ (solid lines), $m_{c,2}$ (dashed lines) and $m_{c,3}$ (dotted lines) vs. $2LU$=$2L(u/r_0)$ with (B) h=0.02 and (D) h=0.1, for various r_0K for Ks=50. The threshold $m_{c,1}$, which separates parameter regimes with bimodal population size distributions (characterised by alternation between the sink state and the large-population state) and unimodal size distributions (populations always in the large-population state) increases with increasing r_0K. The threshold $m_{c,2}$, which separates parameter regimes with bimodal size distributions and unimodal distributions (populations always in the sink state) decreases with increasing r_0K. The threshold $m_{c,3}$, which separates parameter regimes with load greater than or less than the baseline growth rate r_0, increases with increasing r_0K. All predictions are for Ku=0.01.

lower load than island populations) is only effective for very low h; thus, gene flow from the mainland becomes less detrimental to the large-population equilibrium in island populations as h increases. In fact, for $h \gtrsim 0.15$, increasing migration always causes the sink equilibrium to vanish, irrespective of Ks. Moreover, the migration threshold $m_{c,1}$ at which the sink state vanishes becomes lower with increasing h (compare figs. 3(b) and 3(d)). Thus, we observe a genetic Allee effect only at very low migration rates for moderately recessive alleles. This is consistent with the fact that inbreeding load in small populations (due to excess homozygosity) becomes lower as alleles becomes less recessive, and is alleviated by even low levels of migration.

Discussion

A key parameter governing the fate of peripheral populations is $2LU{=}2L(u/r_0)$, the genome-wide deleterious mutation rate relative to the baseline rate of population growth: low-load (large-population) states are possible only for $2LU \lesssim 1$, provided selection against deleterious variants is sufficiently strong and/or migration high. Conversely, for $2LU \gtrsim 1$, populations exist only as demographic sinks, irrespective of selection strength. The parameter $2LU$ is a measure of the 'hardness' of selection and can be small either if the total mutation rate $2Lu$ (which determines total load in the absence of drift) is small or, more realistically, if the growth rate r_0 i.e., the logarithm of the baseline fecundity is high (corresponding to the soft selection limit).

Our analysis highlights qualitatively different effects of migration on population outcomes, depending on fitness effects and the total mutation target of deleterious variants (figs. 2 and 3). For example, with $2LU{=}0.5$ (which corresponds to a $\approx$50% reduction in growth rate due to genetic load in a deterministic population), typical values of Ks must be at least $\sim$5 for recessive and $\sim$10 for additive alleles, if populations are to be metastable in the absence of migration. For selection weaker than this threshold, gene flow from the mainland is beneficial, and aids population survival by hindering the fixation of deleterious alleles. However, for stronger selection and with recessive alleles, the fitness and size of 'low-load' island populations actually declines with increasing migration from the mainland (due to higher deleterious allele frequencies in the latter). In the most extreme scenario, where load is primarily due to segregation of recessive alleles of moderate effect, intermediate levels of migration may actually increase load so much that populations degenerate into high-load demographic sinks (fig. 2(b) and fig. S4 in SI).

We identify two regimes in which peripheral populations can maintain stable numbers at a substantial fraction of carrying capacity, with qualitatively different roles of migration in the two. When selection is strong, i.e., $Ks \gg Ks_c$ (for additive alleles) or $Ks > Ks_{c,2}$ (for recessive alleles) for a given $2LU$, genetic load is low and populations stable, largely independently of migration. In this case, low levels of migration (typically $\lesssim$1 migrant per generation; note typical values of $m_{c,1}$ in fig. 3) are sufficient to prevent a genetic Allee effect, should demographic stochasticity or chance fluctuations in load drive population numbers down. On the other hand, with weakly or moderately deleterious alleles, stable populations rely on rather high levels of migration ($\gg$1 migrant per generation; note typical $m_{c,3}$ in fig. 3) and are only weakly differentiated with respect to the mainland. Here, migration is essential for maintaining heterozygosity and preventing fixation of deleterious alleles, even though numbers are relatively large.

Both classical quantitative genetics and analyses of allele frequency spectra suggest that most mutation load is due to weakly deleterious alleles [23, 24]. The weak selection on deleterious mutations may be strong relative to random drift in the species as a whole [23], but is likely to be dominated by random drift within local demes (i.e., $Ks{<}1$ in our notation). If this is so, then extinction can be avoided only if many migrants enter demes in each generation. Fortunately,

this is generally the case: F_{ST} is typically small (<0.1, say; [25]), implying that m_0>4 (Note that m_0 is the number of migrant genes, corresponding to 2Nm in the usual diploid notation). Thus, whilst selection can act effectively to suppress the mutation load in a well-connected metapopulation, demes that receive few migrants will be vulnerable to the accumulation of load due to weakly selected mutations. Moreover, when fitness has additional environment-dependent components, local adaptation must depend on alleles of intermediate effect and is hindered by high migration, especially for marginal habitats within the metapopulation. [14].

Our analysis has several limitations: first, we ignore environmental stochasticity, which can be an important determinant of population outcomes, especially in parameter regimes where mutation accumulation and demographic stochasticity in themselves are unlikely to lead to extinction [8]. Second, we assume a rather simple architecture of fitness, where genetic load is additive across loci. Deviations from additivity can have a marked influence on purging dynamics [26, 27]. Such deviations may arise, for example, if multiple traits are under stabilizing selection; in this case, segregating variants have deleterious recessive effects on average, even when traits are additive [28]. Finally, we rely on a semi-deterministic analysis, which accounts for genetic drift but neglects demographic stochasticity: while this framework captures various qualitatively different population states across parameter space, it gives little insight into the dynamics. In particular, where alternative — low-load and high-load states are possible, the key assumption underlying the semi-deterministic analysis — namely, that allele frequencies have sufficient time to equilibrate at any given population size, is satisfied only when populations are in one or other state, and not while they transition between states. This makes it challenging to describe the rather complex co-evolution of load and population size during transitions and arrive at a complete understanding of the factors governing transition timescales.

The rather complex effects of migration that emerge even in this relatively simple model with unconditionally deleterious alleles suggest that a comprehensive understanding of the effects of gene flow on eco-evolutionary dynamics at range limits must account for both environment-dependent (local) and environment-independent (global) components of fitness. These may be influenced by (partially) overlapping sets of genetic variants, so that genetic load is shaped fundamentally by pleiotropic constraints. Such extended models are key to understanding when, for example, assisted gene flow is beneficial, and whether its mitigatory effect on inbreeding depression may be outweighed by any outbreeding depression that it might generate.

From a conceptual viewpoint, our analysis highlights the importance of considering explicit population dynamics when analysing the influence of gene flow on the efficacy of selection in small or sub-divided populations. Simple predictions, e.g., that a sub-divided population under hard selection should behave as a single population with an inbreeding coefficient equal to F_{ST} [29, 18], may break down when sub-populations can undergo local extinction. In this case, purging may be ineffective and the efficacy of selection reduced relative to undivided populations, in contrast to standard predictions that subdivision always reduces load when selection is hard. The framework presented here can be extended to metapopulations, thus allowing for a more comprehensive understanding of how the coupled dynamics of population sizes and load influence the fate of fragmented populations.

Funding

This research was partly funded by the Austrian Science Fund (FWF) [FWF P-32896B].

References

[1] Lande R. 1994. Risk of population extinction from fixation of new deleterious mutations. Evolution, vol. 48, no. 5, Oct. 1994, p. 1460. DOI.org (Crossref), doi:10.2307/2410240.

[2] Lynch, M., Conery, J., Bürger, R. (1995), Mutational meltdowns in sexual populations. Evolution, vol. 49, no. 6, Dec. 1995, p. 1067. DOI.org (Crossref), doi:10.2307/2410432.

[3] Frankham, R. (2005) Genetics and extinction. Biological Conservation, vol. 126, no. 2, Nov. 2005, pp. 131–40. DOI.org (Crossref), doi:10.1016/j.biocon.2005.05.002.

[4] O'Grady, J.J., Brook, B.W., Reed, D.H., Ballou, J.D., Tonkyn, D.W., and Frankham, R. (2006) Realistic levels of inbreeding depression strongly affect extinction risk in wild populations. Biological Conservation, vol. 133, no. 1, Nov. 2006, pp. 42–51. DOI.org (Crossref), doi:10.1016/j.biocon.2006.05.016.

[5] Higgins, K., Lynch, M. (2001) Metapopulation extinction caused by mutation accumulation. Proceedings of the National Academy of Sciences of the USA, vol. 98, no. 5, Feb. 2001, pp. 2928–33. DOI.org (Crossref), doi:10.1073/pnas.031358898.

[6] Agrawal, A.F., and Whitlock, M.C. (2011). Inferences about the distribution of dominance drawn from yeast gene knockout data. Genetics, vol. 187, no. 2, Feb. 2011, pp. 553–66. DOI.org (Crossref), doi:10.1534/genetics.110.124560.

[7] Huber, Christian D., Durvasula, A., Hancock, A.M., Lohmueller, K.E. (2018). "Gene Expression Drives the Evolution of Dominance." Nature Communications, vol. 9, no. 1, Dec. 2018, pp. 2750. DOI.org (Crossref), doi:10.1038/s41467-018-05281-7.

[8] Lande, R. (1993). Risks of Population Extinction from Demographic and Environmental Stochasticity and Random Catastrophes. The American Naturalist, vol. 142, no. 6, Dec. 1993, pp. 911–27. DOI.org (Crossref), doi:10.1086/285580.

[9] Lande, R. (1988). Genetics and Demography in Biological Conservation. Science, vol. 241, no. 4872, Sept. 1988, pp. 1455–60. DOI.org (Crossref), doi:10.1126/science.3420403.

[10] Ovaskainen, O., and Hanski, I. Extinction Threshold in Metapopulation Models. Annales Zoologici Fennici, vol. 40, no. 2, 2003, pp. 81-97.

[11] Gyllenberg, M., Hanski, I. Single-species metapopulation dynamics: A structured model. Theoretical Population Biology, vol. 42, no. 1, Aug. 1992, pp. 35–61. DOI.org (Crossref), doi:10.1016/0040-5809(92)90004-D.

[12] Lande, R., Engen, S., and Saether, B.-E. 1998. Extinction times in finite metapopulation models with stochastic local dynamics. Oikos, vol. 83, no. 2, Nov. 1998, p. 383. DOI.org (Crossref), doi:10.2307/3546853.

[13] Ronce, O., and Kirkpatrick, M. 2001. When sources become sinks: migrational meltdown in heterogeneous habitats. Evolution, vol. 55, no. 8, Aug. 2001, pp. 1520–31. DOI.org (Crossref), doi:10.1111/j.0014-3820.2001.tb00672.x.

[14] Szép, E., Sachdeva, H. and Barton, N.H. (2021), Polygenic local adaptation in metapopulations: A stochastic eco-evolutionary model. Evolution, vol. 75, no. 5, May 2021, pp. 1030–45. DOI.org (Crossref), doi:10.1111/evo.14210.

[15] Bell, G., and Gonzalez, A. 2011. Adaptation and evolutionary rescue in metapopulations experiencing environmental deterioration. Science, vol. 332, no. 6035, June 2011, pp. 1327–30. DOI.org (Crossref), doi:10.1126/science.1203105.

[16] Uecker, H., Otto, S.P., and Hermisson, J. 2014. Evolutionary rescue in structured populations. American Naturalist, vol. 183, no. 1, Jan. 2014, pp. E17–35. DOI.org (Crossref), doi:10.1086/673914.

[17] Bridle JR, Vines TH. 2007 Limits to evolution at range margins: when and why does adaptation fail? Trends Ecol. Evol. vol. 22, no. 3, Mar. 2007, pp. 140–47. DOI.org (Crossref), doi:10.1016/j.tree.2006.11.002.

[18] Whitlock, M.C. (2002), Selection, Load and Inbreeding Depression in a Large Metapopulation. Genetics, vol. 160, no. 3, Mar. 2002, pp. 1191–202. DOI.org (Crossref), doi:10.1093/genetics/160.3.1191.

[19] Roze, D. 2015. Effects of interference between selected loci on the mutation load, inbreeding depression and heterosis. Genetics, vol. 201, no. 2, Oct. 2015, pp. 745–57. DOI.org (Crossref), doi:10.1534/genetics.115.178533.

[20] Lenormand, T., Gene flow and the limits to natural selection. Trends in Ecology and Evolution, vol. 17, no. 4, Apr. 2002, pp. 183–89. DOI.org (Crossref), doi:10.1016/S0169-5347(02)02497-7.

[21] Kawecki, T.J. 2008. Adaptation to marginal habitats.Annual Review of Ecology, Evolution, and Systematics, vol. 39, no. 1, Dec. 2008, pp. 321–42. DOI.org (Crossref), doi:10.1146/annurev.ecolsys.38.091206.095622.

[22] Barton, N.H., and Etheridge, A.M. 2018. Establishment in a new habitat by polygenic adaptation. Theor. Popul. Biol, vol. 122, July 2018, pp. 110–27. DOI.org (Crossref), doi:10.1016/j.tpb.2017.11.007.

[23] Charlesworth, B., 2015 The causes of natural variation in fitness– evidence from studies of Drosohila populations. Proceedings of the National Academy of Sciences (U.S.A.), vol. 112, no. 6, Feb. 2015, pp. 1662–69. DOI.org (Crossref), doi:10.1073/pnas.1423275112.

[24] Charlesworth, B., 2018 Mutational load, inbreeding depression and heterosis in subdivided populations. Mol. Ecol. vol. 27, no. 24, Dec. 2018, pp. 4991–5003. DOI.org (Crossref), doi:10.1111/mec.14933.

[25] Morjan C.L., Rieseberg L.H., 2004 How species evolve collectively: implications of gene flow and selection for the spread of advantageous alleles. Mol. Ecol. vol. 13, no. 6, Mar. 2004, pp. 1341–56. DOI.org (Crossref), doi:10.1111/j.1365-294X.2004.02164.x.

[26] Kimura, M., and Maruyama, T. (1966). The mutational load with epistatic gene interactions in fitness. Genetics, vol. 54, no. 6, Dec. 1966, pp. 1337–51. DOI.org (Crossref), doi:10.1093/genetics/54.6.1337.

[27] Kondrashov, A.S (1988). Deleterious mutations and the evolution of sexual reproduction. Nature, vol. 336, no. 6198, Dec. 1988, pp. 435–40. DOI.org (Crossref), doi:10.1038/336435a0.

[28] Abu Awad D., Roze D., 2018. Effects of partial selfing on the equilibrium genetic variance, mutation load, and inbreeding depression under stabilizing selection. Evolution, vol. 72, no. 4, Apr. 2018, pp. 751–69. DOI.org (Crossref), doi:10.1111/evo.13449.

[29] Caballero, A., Keightley, P.D. and Hill, W.G. 1991 Strategies for increasing fixation probabilities of recessive mutations. Genet. Res. vol. 58, no. 2, Oct. 1991, pp. 129–38. DOI.org (Crossref), doi:10.1017/S0016672300029785.

SUPPLEMENTARY INFORMATION
Genetic load and extinction in marginal populations: the role of migration, drift and demographic stochasticity

Himani Sachdeva[1,2,§], Oluwafunmilola Olusanya[1], and Nick Barton[1]

[1]Institute of Science and Technology Austria, Am Campus 1, Klosterneuburg 3400, Austria.
[2]Department of Mathematics, University of Vienna, Vienna 1090, Austria.
[§]*Corresponding author*

A. Description of simulations

We carry out two kinds of simulations: simulations assuming LE (linkage equilibrium) and zero inbreeding, which only track allele frequencies at the L loci and population size N as a function of time; and individual-based simulations, which make no simplifying assumptions and track whole diploid genomes (with L loci) of all individuals present in the island population.

Simulations assuming LE and zero inbreeding. If recombination is faster than all ecological and evolutionary processes, then statistical associations between allelic states at different loci (linkage disequilibria or LD) can be neglected. In addition, if there is no significant inbreeding, then the probability of identity by descent at a locus, and correlations between identity by descent across loci (identity disequilibria or ID) are also negligible. Then, individual genotypes are simply random assortments of deleterious and wildtype alleles, and can be generated by independently assigning alternative allelic states to different loci with probabilities equal to the allele frequencies, allowing us to only track allele frequencies (instead of genotypes).

We initiate simulations by assuming that there are K individuals on the island and that the deleterious allele at each locus is absent. We then evolve the population in discrete time by updating allele frequencies and population size in each generation to reflect the effects of migration, mutation, selection and reproduction, and genetic drift. Starting with frequencies $\{p_j(t)\}$ and size $n(t)$ at the end of generation t, we first implement migration in generation $t+1$ by sampling the number of migrants m from a Poisson

distribution with mean m_0. The population size and allele frequencies are then updated as: $p'_j = \frac{n(t)\,p_j(t) + m\,p_j^{(m)}}{n(t)+m}$ and $n' = n(t)+m$. Here, $p_j^{(m)}$ are the corresponding frequencies on the mainland.

Mutation has no effect on population size: $n''=n'$; allele frequencies are changed as: $p''_j = (1-\mu)p'_j + \mu(1-p'_j)$.

The effects of selection and reproduction are then captured by changing allele frequencies according to: $p'''_j = p''_j + \frac{p''_j[p''_j e^{-s} + q''_j e^{-hs}]}{\overline{w}_j}$, where $\overline{w}_j = q''^2_j + 2p''_j q''_j e^{-hs} + p''^2_j e^{-s}$ and $q''_j = 1 - p''_j$. This is the standard equation relating allele frequencies before and after selection; it assumes that loci evolve independently (no indirect selection due to LD and ID), and that there is no inbreeding. The new population size n''' after selection and reproduction is generated by drawing a Poisson-distributed random variable with mean $n'' e^{r_0(1-n''/K)}\overline{W}$, where the mean population fitness $\overline{W}$ is calculated by multiplying the marginal mean fitnesses of all loci: $\overline{W} = \prod_{j=1}^{L} \overline{w}_j$. Note that sampling the population size from a Poisson distribution (rather than simply choosing it to be equal to the mean of the distribution) introduces demographic stochasticity into the simulation.

The new population size at the end of generation $t+1$ is just: $n(t+1) = n'''$. The new allele frequencies $\{p_j(t+1)\}$ are generated by drawing Binomially distributed random variables $\{X_j\}$ with corresponding parameters $n(t+1)$ and $\{p'''_j\}$ and then setting $\{p_j(t+1)\} = \{X_j/n(t+1)\}$. This last step, which amounts to standard Wright-Fisher sampling of the new allele frequencies based on the new population size $n(t+1)$ and the deterministic allele frequencies p'''_j, 'adds' the random effects of genetic drift on to the systematic effects of migration, mutation and selection (which are already captured by p'''_j).

The procedure described above updates $\{p_j\}$ and n over discrete generations by implementing the effects of migration, mutation, selection and drift in each generation sequentially. An alternative would be to numerically integrate the continuous time equations (eq. 1 in the main text). This is, however, prone to numerical error, and is computationally far more intensive. Both procedures are expected to yield very similar results if $m_0/n, \mu, s, r_0 \ll 1$.

While the allele frequency simulations described here are fast, a fundamental limitation is that the underlying assumptions (i.e., no significant inbreeding, and effects of drift and migration weaker than those of recombination) must break down close to extinction thresholds. Thus, we also carry out individual-based simulations (described below), that make no such assumptions and capture the evolution of all multi-locus associations.

Individual-based simulations. In this bottom-up simulation approach, we track eco-evolutionary dynamics in peripheral populations by explicitly following individuals, recording their allelic states and population numbers from one generation to another. Besides the advantage that comes from inclusion of individual variations and interactions, this modeling framework allows us track the evolution of each locus as well as all the associations among loci (i.e. LD and ID).

We simulate a sexually reproducing population with random mating and non-overlapping discrete generations. At the start of the simulation, the island population is assumed to

consist of N diploid individuals where the fitness of each individual is determined by l loci with two possible allelic state per locus coded by 1's and 0's. The 1 allele is considered the wildtype and the 0 allele the recessive deleterious variant so that the fitness of the three possible genotypes (11, 10 and 00) at each locus are respectively in the ratio $1{:}1-hs{:}1-s$ where s is the homozygous selective effect and h is the dominance coefficient affecting the expression of the deleterious allele. We assume multiplicative fitness across loci (i.e. no epistasis) so that the fitness of an individual with n heterozygous loci can be expressed as $(1-hs)^n(1-s)^{l-n}$. The simulation is initialized by assuming that individuals are initially perfectly fit (i.e are composed of only the 0 allelic state) so that the frequency of the deleterious variant at each locus is 0. The order of events in the life cycle of individuals in each generation is taken as, mutation $\rightarrow$ migration $\rightarrow$ reproduction (meiosis and genetic recombination)+ density-dependent survival. These would be explained in a little more detail below.

Mutation: We model both forward and backward mutation rates i.e. with probability μ, there is a shift from an allelic state 1 to 0 and with probability ν there is a shift in the opposite direction. In this work, we assumed $\mu{=}\nu$ although this is not true in general.

Migration: the migration step is implemented by choosing a random number, of individuals (drawn from a Poisson distribution with rate m_0) to be migrants from a fixed mainland pool assumed to be in deterministic mutation-selection balance. Allelic states are then randomly assigned to each migrant locus such that the frequency of the deleterious variants (among migrants) at each locus are close to the deterministic predictions for a single locus under mutation-selection balance. Following migration, both the frequency at each locus as well as the population size on the island change.

Reproduction+density dependent survival: This phase of the simulation involves gamete formation (through the process of meiosis and genetic recombination) as well as a decision as to how many offspring survive to be parents in the next generation. The latter is done by sampling an integer number, l say, from a Poisson distribution with rate $N'\overline{W}e^{r_0\left(1-\frac{N'}{K}\right)}$ where K is the carrying capacity of the population, N' is the population size after migration, $\overline{W}$ is the mean fitness of the population and r_0 the population growth rate. Once this is determined, l pairs of parents are then selected (with replacement) from the population in proportion to their fitness to form offspring individuals. Each offspring gamete is formed by assuming that the allelic state contributed to the gamete at any given locus is sampled from the same or alternative chromosome in both parents with probability 0.5 (i.e. free recombination).

B. Semi-deterministic approximation

The semi-deterministic approximation outlined in the main text applies when the distribution of population sizes is sharply peaked around one or more values. For a given set of parameters Ks, Ku, h, $2LU{=}2L(u/r_0)$, and m_0, we expect the peaks of the distribution to become sharper and the predictions of the semi-deterministic approximation to become more accurate for larger r_0K (corresponding to weaker demographic fluctuations) and larger L (corresponding to weaker fluctuations in genetic load). Figure S1a illustrates this by plotting the distribution $P(N)$ (as obtained from allele frequency simulations) for

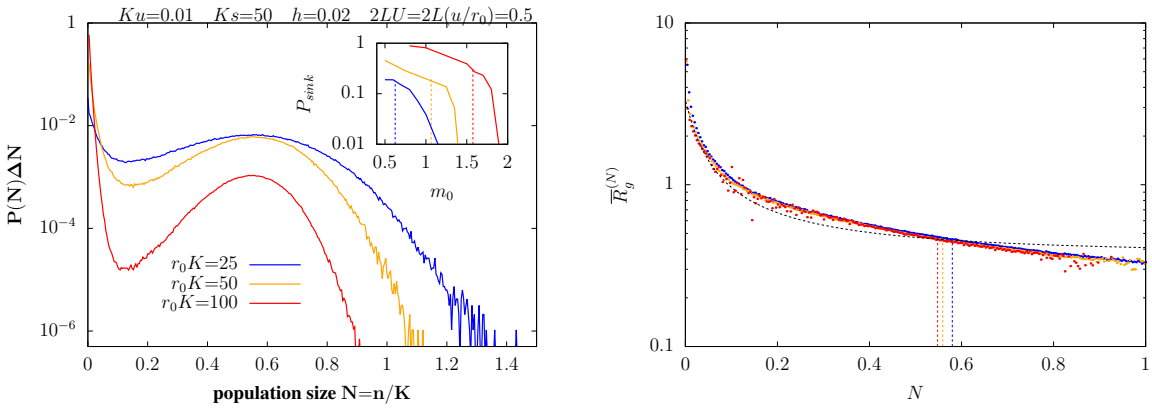

(a) (b)

Figure S1: (A) Distribution of population sizes $P(N)$ integrated over intervals of size ΔN=0.004 for r_0K=25, 50, 100 (blue, orange, red), where r_0K is varied by changing K (along with s, u, L), while keeping Ku, Ks, $2LU$=$2L(u/r_0)$ and r_0 constant. Inset: P_{sink}, the probability that the population is in the sink state, vs. m_0, the number of migrants per generation. Vertical dashed lines represent semi-deterministic predictions for the critical threshold $m_{c,1}$, at which the sink equilibrium vanishes. P_{sink} is calculated by integrating the distribution $P(N)$ from 0 to the minimum of the distribution (which lies between the sink and large-population equilibrium). (B) Average load $\overline{R_g^{(N)}}=\int R_g P[R_g, N]\, dR_g$ at a given N (points; different colours correspond to different r_0K) and the expected load under mutation-selection-drift equilibrium for that N (dashed line) as a function of N. Average load equals the equilibrium expectation at the predicted large-population equilibrium (indicated by vertical dashed lines) for all r_0K; the two quantities also match closely near N=0 for larger values of r_0K. All results (solid lines in A and points in B) are from allele frequency simulations; dashed lines indicate various semi-deterministic predictions (as described above). Parameter values: Ku=0.01, Ks=50, h=0.02, $2LU$=$2L(u/r_0)$=0.5 and r_0=0.1.

various values of r_0K (which is changed by changing K). Note that in increasing K, while holding Ks, Ku and $2L(u/r_0)$ constant, we must simultaneously lower s and u, while increasing L proportionately.

As expected, the peak corresponding to the large-population equilibrium becomes narrower, i.e., typical fluctuations in N about the average (in that state) become smaller, as r_0K increases. The distribution of population sizes in the sink state also becomes more sharply clustered around 0, and the valley separating the large-population equilibrium from the sink state becomes deeper as r_0K increases.

We then ask whether the basic approximation underlying the semi-deterministic analysis– that genetic load is close to its equilibrium expectation under drift-mutation-migration-selection balance when populations are in one or other metastable state– becomes increasingly accurate for larger r_0K. Figure S1b shows the average load $\overline{R_g^{(N)}}=\int R_g P[R_g, N]\, dR_g$ at a given N (as obtained from allele frequency simulations), as a function of N for various r_0K. The average load (points) is different from the load expected under mutation-selection-drift-migration balance $\mathbb{E}[R_g|N]$ (black line) except under two conditions: first, the average load equals the equilibrium expectation near the large-population equilibrium (indicated by vertical dashed lines) for all values of r_0K (different colours); second, the average load also matches the equilibrium expectation in the vicinity of N=0 for large r_0K.

These observations are consistent with the general expectation that allele frequencies and genetic load will equilibrate only if population sizes remain roughly constant over the time scales required to reach mutation-selection-drift-migration balance: this condition can only be satisfied close to the peaks of the distribution (which correspond to equilibria of the semi-deterministic population size dynamics) and will typically not hold while populations transition between equilibria. A priori, it is unclear whether this condition is even satisfied in the sink state, in which N exhibits fluctuations that are large (relative to the mean) and characterised by significant skew towards small sizes. Figure S1b suggests that it may nevertheless be reasonable to approximate the average load in the sink state by the equilibrium expectation, at least for large values of r_0K.

Accordingly, we note that the accuracy of the semi-deterministic prediction for the critical migration threshold, $m_{c,1}$, at which the sink state vanishes, improves with increasing r_0K. This is illustrated in the inset of fig. S1a, which shows P_{sink}, the probability that the population is in the sink state (as observed in simulations) against m_0. The semi-deterministic prediction for $m_{c,1}$ (vertical dashed lines) approaches the corresponding threshold in simulations (where P_{sink} goes to 0) as r_0K increases.

Semi-deterministic prediction for $m_{c,1}$ in the $r_0K\to\infty$ limit. In order to obtain the semi-deterministic prediction for the population size, genetic load and expected allele frequencies at one or more equilibria, we numerically solve for the $\{N_*\}$ satisfying:

$$N_*\,(1-N_*-\mathbb{E}[R_g|N_*])+M_0=0 \qquad \text{where} \quad \mathbb{E}[R_g|N_*]=\sum_j S_j[\mathbb{E}(p_j|N_*)+(2h_j-1)\mathbb{E}(p_jq_j|N_*))] \tag{S1}$$

where the expectations are obtained by integrating over the equilibrium allele frequency distributions (eq. 2 of the main text). The equation above is the same as eq. 3 of the main text. An equilibrium N_* is a stable equilibrium if the function $N\,(1-N-\mathbb{E}[R_g|N])+M_0$ has a negative derivative with respect to N at $N=N_*$.

In the limit $r_0K\to\infty$, $L\to\infty$, $s\to0$, $u\to0$, with m_0, Ks, Ku and $2LU=2L(u/r_0)$ constant, the demographic contributions of migration, represented by the $M_0=m_0/r_0K$ term in the above equation, can be neglected, yielding $N_*\,(1-N_*-\mathbb{E}[R_g|N_*])=0$. This function (which must be zero at equilibrium) is plotted as a function of population size in fig. S2a for three different levels of migration (which influence the function via the term $\mathbb{E}[R_g|N_*]$). There is always an equilibrium ($N=0$) at extinction; this equilibrium is stable if the curve is downward sloping at $N=0$, i.e., if $1-\lim_{N_*\to0}\mathbb{E}[R_g|N_*]<0$. In addition, there may be two other equilibria— one stable and the other unstable— satisfying $N_*=1-\mathbb{E}[R_g|N_*]$. For low $2LU$ and/or h not too low, an increase in migration causes the sink equilibrium to become unstable, so that above a critical migration threhsold $m_{c,1}$, only a single, stable 'large-population' equilibrium exists.

In the limit $r_0K\to\infty$, the change in the stability properties of the sink equilibrium occurs at the migration rate for which $\lim_{N_*\to0}\mathbb{E}[R_g|N_*]=1$. Since $\lim_{N_*\to0}\mathbb{E}[R_g|N_*]$, the expected load in the limit $N_*\to0$, depends only on the neutral allele frequency and neutral heterozygosity under migration-drift balance, we can obtain an explicit expression that depends on LS,

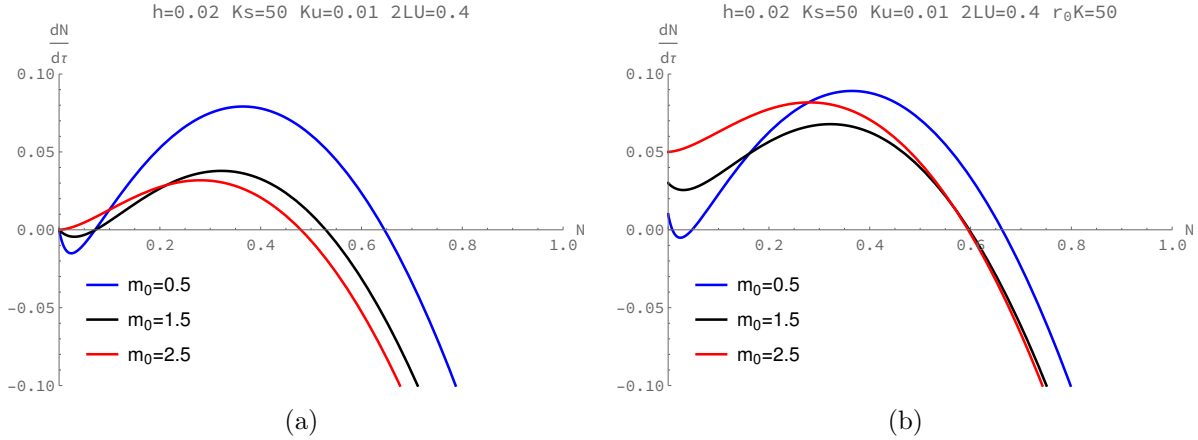

Figure S2: (A)-(B) Rate of change of population size N under the semi-deterministic approximation (eq. (S1)) as a function of N (A) in the $r_0K\to\infty$ limit (where the demographic effects of migration, represented by the M_0 term, can be neglected) (B) for finite r_0K (i.e., including the M_0 term). Equilibria correspond to points at which the curves cross the horizontal (zero growth rate axis); stable equilibria are those for which the curves have a negative slope at the point of zero crossing. Parameter values (Ks=50, Ku=0.01, $2LU$=0.4 and h=0.02 in A and B; r_0K=50 in B) correspond to a regime where increasing migration causes the extinction fixed point to become unstable (in the $r_0K\to\infty$ limit; fig. A) or the sink fixed point to vanish (for finite r_0K; fig B).

h, $p^{(m)}$ and m_0. Finally, setting $\lim_{N_*\to 0}\mathbb{E}[R_g|N_*]=1$ and solving for the number of migrants per generation yields:

$$m_{c,1}=\frac{LSp^{(m)}-1}{4[1-LSp^{(m)}(p^{(m)}+2h(1-p^{(m)}))]} \tag{S2}$$

which is eq. 4 of the main text.

In order to illustrate the effects of the demographic term on equilibria and their stability properties, we also plot $N\,(1-N-\mathbb{E}[R_g|N])+M_0$ (eq. (S1) including the M_0 term) as a function of N (fig. S2b). At low migration levels, there is a sink equilibrium (with N_* close to but not equal to zero) and a large-population equilibrium. Increasing migration now causes the sink equilibrium to vanish, rather than rendering it unstable. The critical threshold $m_{c,1}$ in this case is significantly lower than the $r_0K\to\infty$ prediction above (see also fig. 3B of the main text), highlighting how, migration can influence population outcomes via both genetic and demographic effects.

C. Comparison of individual-based simulations with simulations under LE and IE

Here we compare results from the two simulation approaches by looking at the effect of migration on the mean population size and mean genetic load at equilibrium (fig. S3a – S3c) as well as on the stochastic distribution of population size (fig. S3d – S3f) on the island under different genetic architectures i.e. for weakly deleterious alleles ($Ks<Ks$; left column), mildly or moderately deleterious alleles ($Ks\gtrsim Ks_c$; middle column) and strongly deleterious alleles ($Ks\gg Ks_c$; right column).

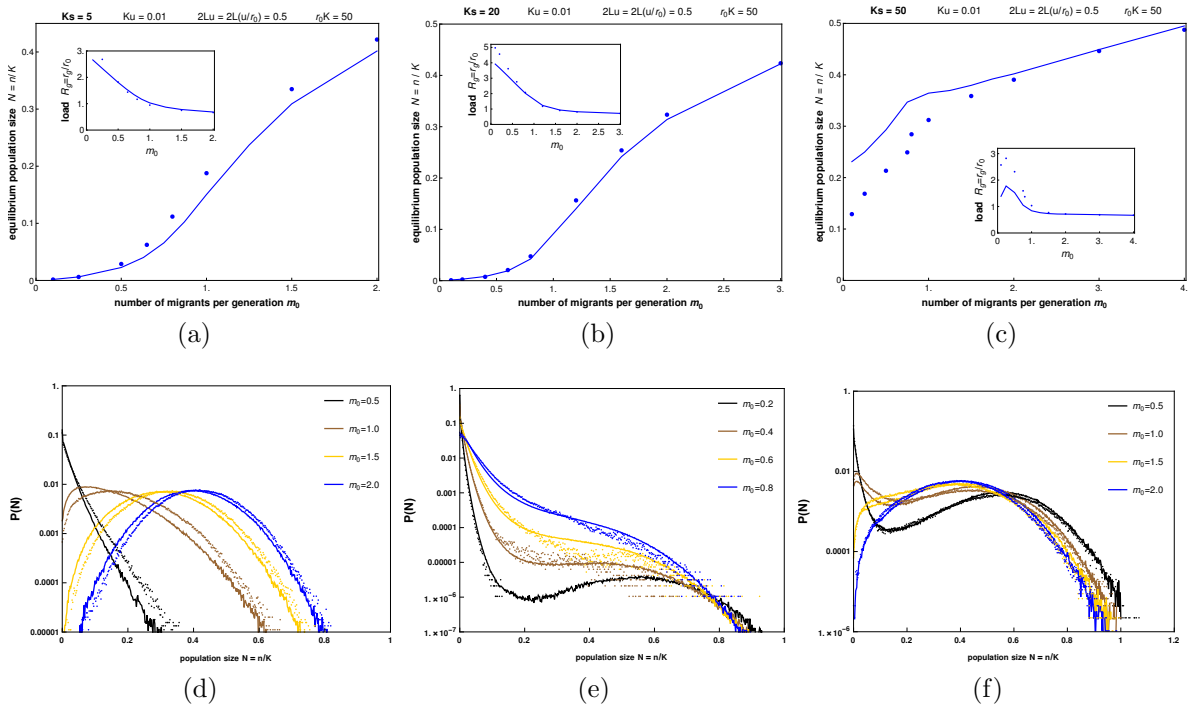

Figure S3: (A)-(C) Mean population size (main figure) and mean genetic load (inset) at equilibrium plotted against m_0 (the number of migrants per generation) for weakly deleterious ($Ks<Ks_c$; left column), mildly deleterious ($Ks\gtrsim Ks_c$; middle column) and strongly deleterious ($Ks\gg Ks_c$; right column) nearly recessive alleles. Solid lines represent result obtained from allele frequency simulations (assuming LE and zero inbreeding) while dots represent result from individual-based simulations. (D)-(F) Equilibrium probability distribution of scaled population sizes $N=n/K$ for various values of m_0, as obtained from simulations assuming LE and IE (solid lines) as well as from individual based simulations (dots) under the three parameter regimes.

Weakly deleterious nearly recessive alleles (left column of fig. S3): For $Ks<Ks_c$, the population approaches extinction for low migration. However, increasing migration causes an increase in the size of the island population (main plot of fig. S3a) as well as a corresponding decrease in the genetic load (inset). This is true for both types of simulations although the individual based simulation (dots) produces slightly higher population numbers with increasing m_0. Looking at the stochastic distribution of population size (fig. S3d), populations exhibit a single stable equilibrium for all migration rates and shift to the right towards increasing N (following a Gaussian distribution centered around the stable equilibrium) as m_0 increases. As noticed in fig. S3a, there exists a slight difference between both simulation approaches, namely that the individual based simulation produces slightly higher numbers (see dotted plots in fig. S3d). This suggests that LD can cause a somewhat higher increase in population size by its purging effect on sets of locally maladapted alleles.

Moderately deleterious nearly recessive alleles (middle column of fig. S3): Just as with weakly deleterious alleles, an increase in migration increases the population size (main plot of fig. S3b) and reduces the genetic load (inset) on the island, although we observe a higher load for low values of migration in the individual based simulation.

Looking at fig. S3e, the individual based simulation breaks down for very low migration rates as it requires extremely long simulation runs (both time and memory consuming) to observe the peak at the large population state equilibrium (see LE simulations - solid lines).

Strongly deleterious nearly recessive alleles (right column of fig. S3): For $Ks \gg Ks_c$, we observe an initial sharp increase in population size with m_0. Beyond m_0=1, the population size increases further but with a less steep slope. Similarly, for very low m_0, the genetic load in the population increases initially and then falls sharply with increasing m_0 after which it approaches a steady value. Interestingly, for low migration rates, individual based simulations slightly diminish the population size and increase the load (see blue dots) suggesting a negative effect of LD on strongly deleterious alleles when migration is low. From fig. S3f, we observe a bimodal distribution of population size (with one peak close to extinction and the other close to the deterministic equilibrium) when migration is rare. However, with increasing migration, there is a shift from the bimodal to a unimodal population size distribution.

D. Evolutionary outcomes with a distribution of fitness effects

In the main text, we analyse scenarios where all deleterious variants have equal selective effects and dominance coefficients, and illustrate how migration may have qualitatively different effects, depending on the magnitude of the homozygous selection coefficient, dominance coefficient and the total mutation rate. Here, we ask: what is the effect of migration on population outcomes when the genetic load is due to loci with a distribution of fitness effects? For the purposes of illustration, we consider a somewhat artificial distribution where a fraction α of loci are subject to deleterious mutations that are nearly recessive (h_R=0.02) with scaled selection coefficient Ks_R, and the remaining fraction $1-\alpha$ are additive (h_A=0.5) with scaled selective coefficient Ks_A. Thus, the mutation targets for the two types of deleterious variants are $2L\alpha U$ and $2L(1-\alpha)U$ respectively.

If recessive variants are weakly deleterious (Ks_R less than the corresponding critical threshold Ks_c), then their contribution to genetic load will decrease with increasing migration. Since migration always reduces additive load (though only marginally for $Ks_A \gg 1$), the net effect of increasing migration in this case is to reduce load and increase the equilibrium population size (results not shown). We thus focus on recessive alleles with moderate or strongly deleterious effects ($Ks_R > Ks_c$), where an increase in recessive load with increasing migration can potentially counteract a reduction in additive load. Figures S4a-S4c show semi-deterministic predictions for equilibrium population sizes versus m_0 for various combinations of Ks_A and Ks_R for α=0.1 (predominantly additive load), 0.5 (nearly equal contributions of additive and recessive alleles to load) and 0.9 (load primarily due to recessive alleles). Where two stable equilibria exist, these are shown by solid and dashed lines (of the same color).

We observe a genetic Allee effect (characterised by the co-existence of alternative 'sink' and 'large-population' equilibria) at low migration rates for all parameter combinations, except when load is primarily due to weakly deleterious additive alleles (red and brown

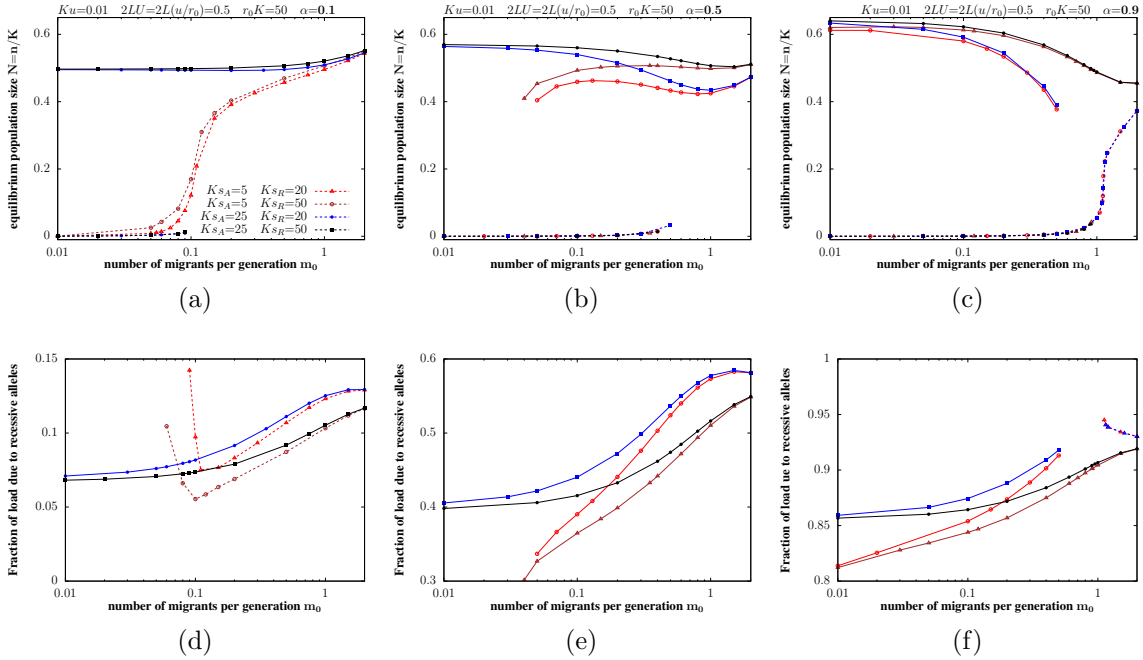

Figure S4: (A)-(C) Semi-deterministic predictions for population size(s) at equilibrium vs. m_0, the number of migrants per generation. Different colors correspond to different values of Ks_A and Ks_R, the (scaled) homozygous selection coefficients for the additive (h=0.5) and nearly recessive (h=0.02) alleles (see legend of fig. A). We depict cases where a fraction α of alleles have nearly recessive effects and the remaining fraction $1-\alpha$ additive effects, for α=0.1 (left), α=0.5 (middle) and α=0.9 (right). Where two alternative equilibria exist, these are shown by solid and dashed lines (of the same color). (D)-(F) Semi-deterministic predictions for the fraction of the total load that is due to recessive alleles vs. m_0, for parameter combinations where the total load is less then r_0, i.e., where the population is not a sink. Where two equilibria with load less than r_0 exist, the fractions corresponding to each are depicted by solid and dashed lines. All figures show results for: Ku=0.01, $2LU$=0.5, r_0K=50.

curves in fig. S4a). Increasing migration tends to destabilize the sink state in all cases, except where load is largely due to recessive alleles with moderately deleterious effects (red and blue curves in fig. S4c): in this extreme limit, it is the large-population state that vanishes at high migration levels (see also fig. 2C, main text). The critical migration threshold at which the sink state vanishes (and Allee effects no longer occur) is higher when the contribution of recessive alleles to total load is higher (α larger) and homozygous effects associated with recessive alleles more moderate. The population size associated with the large-population equilibrium increases marginally with increasing migration for small α (as expected when load is predominantly additive), decreases with increasing migration for large α (as expected when load is predominantly recessive), and exhibits a weak, non-monotonic dependence on m_0 for intermediate α (reflecting the opposing effects of migration on additive and recessive alleles).

We also track how the relative contributions of additive and recessive alleles to total load change with increasing migration. Figures S4d-S4f shows the fraction of total load that is due to recessive alleles vs. m_0, for parameter combinations where the population is not a sink, i.e., where the total load is less than the baseline growth rate r_0. This fraction increases with increasing m_0 in all cases (except when the population is close to a sink state, i.e., $R_g\sim1$), with the most significant increase occurring for α=0.5, and

where additive alleles have weak effects and recessive alleles moderate effects. Under these conditions, smaller isolated populations (with low migration) can more efficiently purge recessive load, but maintain higher levels of additive load. An increase in migration tends to decrease the additive load and increase the recessive load by pushing the frequencies of deleterious additive and recessive alleles closer to the mainland values (that are respectively lower and higher than those on the island).

Note that in this case, the total load and population size do not change significantly with migration (because of the opposing effects of migration on the two components of load). The change in the relative contributions of different kinds of alleles may nevertheless have significant consequences, by making populations with higher levels of migration (and accordingly, a greater number of segregating recessive alleles) more vulnerable to future extinction, e.g., in the event of a bottleneck.